# OBP-801, a novel histone deacetylase inhibitor, induces M-phase arrest and apoptosis in rhabdomyosarcoma cells

CHIHIRO TOMOYASU[1*], KEN KIKUCHI[1,2*], DAISUKE KANEDA[1], SHIGEKI YAGYU[1], MITSURU MIYACHI[1], KUNIHIKO TSUCHIYA[1], TOMOKO IEHARA[1], TOSHIYUKI SAKAI[3] and HAJIME HOSOI[1]

[1]Department of Pediatrics, Graduate School of Medical Science, Kyoto Prefectural University of Medicine, Kyoto 602-8566; [2]Department of Pediatrics, Uji Takeda Hospital, Kyoto 611-0021; [3]Department of Molecular-Targeting Cancer Prevention, Kyoto Prefectural University of Medicine, Kyoto 602-8566, Japan

Received May 18, 2018; Accepted October 11, 2018

DOI: 10.3892/or.2018.6813

**Abstract.** Rhabdomyosarcoma (RMS) is an aggressive pediatric cancer of musculoskeletal origin. Despite multidisciplinary approaches, such as surgical resection, irradiation, and intensive chemotherapy, adopted for its treatment, the prognosis of patients with high-risk RMS remains poor. Thus, molecularly targeted therapies are required to improve patient survival and minimize side effects. Histone deacetylases (HDACs) modify transcription by deacetylation of the lysine residues in chromatin histone tails and several non-histone proteins. HDAC inhibitors, classes of compounds targeted to various HDAC proteins, are being studied for their roles in several types of cancers in a rigorous manner. This study aimed to investigate the potential of a novel HDAC inhibitor, OBP-801, as a therapeutic agent for the treatment of RMS. We used 8 RMS cell lines in this study. Protein expression patterns, cell proliferation, cell cycle status, and apoptosis in RMS cells after OBP-801 treatment *in vitro* were investigated. We also studied the antitumor activity of OBP-801 in an *in vivo* xenograft mouse model. We observed cell cycle arrest at the M-phase and apoptosis in all RMS cell lines after exposure to pharmacological levels of OBP-801 for 24 h. Immunofluorescence staining revealed that OBP-801 may induce mitotic catastrophe via chromosome misalignment and reduced survivin expression, ultimately leading to apoptosis. Our results demonstrated that the novel HDAC inhibitor OBP-801 was an effective inhibitor of RMS cell line proliferation and may be a potent therapeutic option for RMS.

## Introduction

Rhabdomyosarcoma (RMS) constitutes ~60% of all childhood soft tissue sarcomas. It is a small, round-cell tumor of musculoskeletal origin that exhibits various degrees of myogenic differentiation. Most types of RMS fall into 1 of 2 biological distinction subgroups defined as alveolar or embryonal type (1). Alveolar RMS (ARMS), which accounts for 41% of all RMS, is an aggressive soft tissue sarcoma in children, with a high invasion and metastasis at initial diagnosis. Despite a combination therapy, which includes surgical resection, radiation, and intensive chemotherapy, the prognosis for patients with ARMS remains poor (2). Recently, many molecular targeted drugs have been effectively used in patients with different types of tumors; however, for RMS, targeted drugs are still under investigation and have not been used clinically (3-5).

Histone deacetylase (HDAC) inhibitors are promising drugs for the treatment of diverse cancers due to their abilities to induce cell cycle control and apoptosis (6-9). Numerous of HDAC inhibitors are currently being assessed in various phases of clinical trials (10,11). The United States Food and Drug Administration (US FDA) has already approved the HDAC inhibitors belinostat, vorinostat, and romidepsin for the treatment of peripheral and cutaneous T cell lymphoma (12-14). There have been a few studies on the tumor suppressive effects of RMS by HDAC inhibition *in vitro* (15,16). A recent study in an ARMS mouse model revealed that response to the HDAC inhibitor was different depending on the myogenic lineage of the tumor cells (17). Presently, the role of HDAC activity in

*Correspondence to:* Dr Ken Kikuchi, Department of Pediatrics, Graduate School of Medical Science, Kyoto Prefectural University of Medicine, Kajii-cho, Kawaramachi-Hirokoji, Kamigyo-ku, Kyoto 602-8566, Japan
E-mail: ken-k@koto.kpu-m.ac.jp

*Contributed equally

*Abbreviations:* RMS, rhabdomyosarcoma; ARMS, alveolar RMS; HDAC, histone deacetylase; ERMS, embryonal RMS; DMSO, dimethyl sulfoxide; PBS, phosphate-buffered saline; SD, standard deviation; $IC_{50}$, half maximal inhibitory concentration

*Key words:* histone deacetylase inhibitor, rhabdomyosarcoma, apoptosis, cell cycle, cancer therapy

RMS tumorigenesis and the essential mechanisms by which HDAC inhibitors exhibit their antitumor effects remain largely unknown.

OBP-801 (spiruchostatin A) was originally identified as an enhancer of PAI-1 gene expression and was established as a new HDAC inhibitor by a p21 promoter reporter screen (18). OBP-801 exerted the most potent HDAC-inhibitory activity in our study; it was ~50 times more effective than vorinostat (18). It is currently under clinical trials in the United States.

The aim of this study was to evaluate the effect of the new HDAC inhibitor, OBP-801, on the cell cycle control and on the viability of RMS cells *in vitro* and *in vivo* using a mouse tumor model. We also assessed the mechanism of action of OBP-801.

## Materials and methods

*Cell lines and reagents*. We used the human ARMS cell lines SJ-Rh30 (Rh30), SJ-Rh41 (Rh41), SJ-Rh3 (Rh3), SJ-Rh4 (Rh4), SJ-Rh18 (Rh18) and SJ-Rh28 (Rh28) that were kindly provided by Peter J. Houghton M, San Antonio, TX, USA), and the embryonal RMS (ERMS) cell lines RD that was obtained from JCRB (Japanese Collection of Research Bioresources) Cell Bank and RMS-YM that was kindly provided by Naoki Kakazu M.D. (Department of Environmental and Preventive Medicine, Shimane University School of Medicine, Shimane, Japan) (5,19). They were maintained in Dulbecco's modified Eagle's medium (DMEM) supplemented with 10% fetal bovine serum (FBS) at 37˚C in a 5% $CO_2$ incubator. OBP-801 (Oncolys BioPharma, Inc., Tokyo, Japan) was dissolved in dimethyl sulfoxide (DMSO) and stored as a 1-mM stock solution in 50-$\mu$l aliquots at -20˚C. The percentage of DMSO in all experiments was <0.01%.

*Western blot analysis*. Cells were lysed in RIPA buffer (08714-04; Nacalai Tesque, Kyoto, Japan). Protein concentrations in cell lysates were determined using BCA assay. A total of 20 $\mu$g of protein were separated by sodium dodecyl sulfate-polyacrylamide gel electrophoresis (SDS-PAGE) on NuPAGE Novex 4-12% Bis-Tris gels in NuPAGE MES SDS running buffer (Life Technologies; Thermo Fisher Scientific, Inc.). Proteins were subsequently transferred to Immobilon-P membranes in NuPAGE Transfer buffer (Life Technologies; Thermo Fisher Scientific, Inc). Membranes were blocked in phosphate-buffered saline with Tween-20 (PBST) containing 5% non-fat dry milk powder, and then incubated at 4˚C overnight with primary antibodies against the following proteins: anti-histone-H4 (dilution 1:1,000; cat. no. 13919; Cell Signaling Technology, Inc., Danvers, MA, USA), anti-acetyl histone-H4 (dilution 1:1,000; cat. no. 06-866; Merck KGaA, Darmstadt, Germany), anti-Rb (dilution 1:2,000; cat. no. 554136; BD Biosciences, Franklin Lakes, NJ, USA), anti-phospho-histone-H3 (dilution 1:2,000; cat. no. 3377; Cell Signaling Technology, Inc.), anti-survivin (dilution 1:2,000; cat. no. 2808; Cell Signaling Technology, Inc.) and anti-p21 Waf1/Cip1 (1:2,000; cat. no. 2946; Cell Signaling Technology, Inc.), anti-total caspase-3 (dilution 1:2,000; cat. no. 610322; BD Biosciences), anti-cleaved caspase-3 (dilution 1:1,000; cat. no. 9664; Cell Signaling Technology, Inc.) and anti-β-actin (dilution 1:5,000; cat. no. A2228; Merck KGaA) for the reference protein. The membranes were then washed with PBST and incubated at room temperature for 1 h with sheep anti-mouse secondary antibody (dilution 1:10,000; cat. no. NA931; GE Healthcare, Little Chalfont, UK) or donkey anti-rabbit secondary antibody (dilution 1:10,000; cat. no. NA934; GE Healthcare). Antibody binding was detected using the enhanced chemiluminescence detection system (ECL and ECL prime; GE Healthcare) (20). The protein density of western blot was measured by ImageJ 1.52a (National Institutes of Health, Bethesda, MD, USA).

*WST-8 cell viability assay*. We performed WST-8 colorimetric assays with Cell Counting Kit-8 (Nacalai Tesque, Inc.) according to the manufacturer's instructions. We seeded the cells in 96-well plates in 100 $\mu$l culture medium for 24 h, then added various reagents. We determined cell viability by assessing the optical density (OD) at 450 nm with a microplate reader (Multiskan™ JX; Dainippon Sumitomo Pharma Co., Ltd., Osaka, Japan), as previously described (20).

*Cell cycle analysis*. To analyze their cell cycle distribution, we cultured the cells in the presence of OBP-801 or an equivalent volume of DMSO for 24 h. We then isolated the cells by scraping, washed them with phosphate-buffered saline (PBS), and incubated them with propidium iodide at a concentration of 50 $\mu$g/ml for 30 min to stain DNA. We determined their DNA content on a FACSCalibur™ flow cytometer (BD Biosciences). We analyzed their cell cycle status with FlowJo software 7.6.5 (Tree Star, Inc., Ashland, OR, USA), as previously described (21).

*Analysis of apoptosis by flow cytometry*. We analyzed cell death after Annexin V-FITC and propidium iodide staining with a TACS Annexin V-FITC Apoptosis Detection kit (R&D Systems, Inc., Minneapolis, MN, USA), according to the manufacturer's instructions. We analyzed the data with FlowJo software (Tree Star, Inc.) as previously described (21).

*Immunocytochemistry*. We plated the cells on Falcon® 8-Well Culture Slides (cat. no. 354118; BD Falcon; Corning, Inc., Corning, NY, USA), then fixed with 4% paraformaldehyde, permeabilized with 0.1% Triton™ X-100, washed with PBS, and incubated with anti-survivin (dilution 1:1,000; cat. no. 2808), anti-α-tubulin (dilution 1:1,000; cat. no. 3873), anti-phospho-histone-H3 (dilution 1:1,000; cat. no. 3377), or anti-phospho-H2AX (dilution 1:1,000; cat. no. 9718; all from Cell Signaling Technology, Inc.) at 4˚C overnight. We then rinsed the slides with PBS and incubated them with Alexa Fluor 488/555-conjugated anti-mouse/rabbit IgG (dilution 1:200; cat. nos. A11008, A11001 and A21422; Cell Signaling Technology, Inc.) at room temperature for 1 h. Finally, we examined the slides by fluorescence microscopy with a KEYENCE BZ-X700 instrument (Keyence Corp., Osaka, Japan).

*In vivo mouse xenograft studies*. Female BALB/c nu/nu nude mice (4-weeks old, total 14, 11-16 g) were purchased from Japan SLC, Inc. (Shizuoka, Japan). All experiments and procedures were conducted in accordance with the institutional animal care and use committee guidelines. The present study was also approved by the Committee for Animal Research

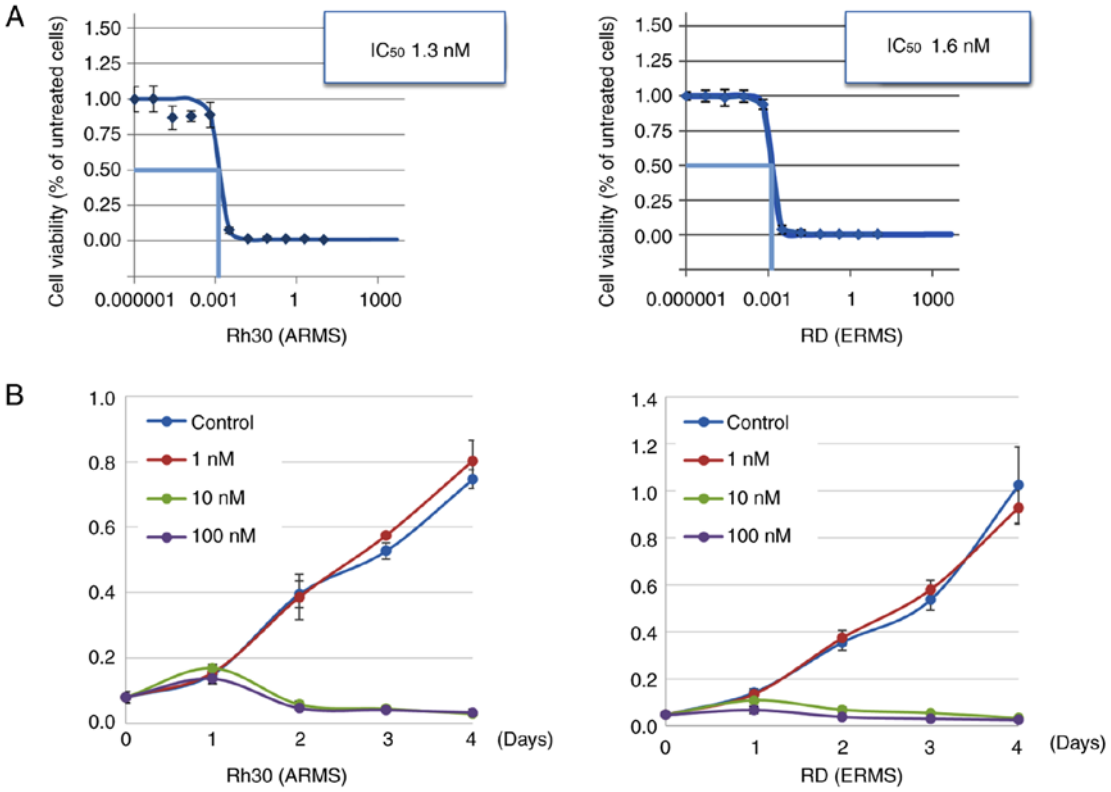


Figure 1. OBP-801 inhibits ARMS and ERMS cell growth *in vitro*. (A) Viability of R30 (ARS) and RD (ERMS) cells assessed by WST-8 assay, after treatment with OBP-801 (range, 0-20 $\mu$M) for 72 h. $IC_{50}$ values were determined for each cell line. The bars indicate the mean ± SD of triplicate independent experiments. (B) Rh30 and RD cells were treated with OBP-801 at various concentrations. We determined the number of cells by WST-8 assay. The bars indicate the mean ± SD of triplicate independent experiments. ARMS, alveolar RMS; ERMS, embryonal RMS.

of Kyoto Prefectural University of Medicine (permission no. M27-477). Mice were maintained at 23±2˚C under a 12-h light/dark cycle (light period, 07:00-19:00 h). Food and water were available *ad libitum*. We subcutaneously injected $1x10^7$ luciferase-positive Rh30 cells into the dorsal area of BALB/c nu/nu nude mice (n=3 and 4/group). We monitored tumor growth in live mice by bioluminescent detection of the luciferase activity of the Rh30 cells at days 3 and 52, as previously described (22). We assessed the tumor sizes twice per week using calipers using the formula $(a \times b^2)/2$. The mice were euthanized by barbiturate overdose.

*Optical imaging for luminescence*. We performed *in vivo* bioluminescence imaging of live mice using a Xenogen IVIS®-Illumina system (PerkinElmer, Inc., Waltham, MA, USA). The animals were maintained under inhaled anesthesia (2% isoflurane in 100% oxygen at the rate of 2.5 l/min). For imaging of the firefly luciferase reporter harbored by the tumor cells, we administered a single luciferin dose of 150 mg/kg (PerkinElmer, Inc.) via intraperitoneal injection 20 min prior to imaging. The data were acquired and analyzed using the manufacturer's proprietary Living Image software 4.4 (PerkinElmer, Inc.).

*Statistical analysis*. Average values were expressed as the mean ± standard deviation (SD). We used the 2-tailed Student's t-test for comparison of the means between groups. Differences with a P-value of <0.05 were considered to indicate a statistically significant difference.

Table I. The half maximal inhibitory concentrations of OBP-801 in the various RMS cell lines.

| Cell line | Tumor type | $IC_{50}$ (nM) |
|---|---|---|
| RD | ERMS | 2.5±1.4 |
| RMS-YM | ERMS | 2.7±0.3 |
| Rh30 | ARMS | 1.5±0.8 |
| Rh41 | ARMS | 2.5±0.9 |
| Rh3 | ARMS | 0.7±0.4 |
| Rh4 | ARMS | 2.2±1.0 |
| Rh18 | ARMS | 2.6±0.8 |
| Rh28 | ARMS | 0.9±0.7 |

The experiment was performed in triplicate and the half maximal inhibitory concentrations ($IC_{50}$) are shown as the mean ± SD (n=3). RMS, rhabdomyosarcoma.

## Results

*OBP-801 inhibits the growth of RMS cell lines*. We examined the effect of the HDAC inhibitor OBP-801 on the growth of ERMS and ARMS cell lines. The mean half maximal inhibitory concentration ($IC_{50}$) values were 2.6±0.2 nM for the ERMS cells and 1.8±0.8 nM for the ARMS cells (Table I). OBP-801 inhibited the growth of RD and Rh30 in a concentration- and time-dependent manner (Fig. 1A and B).

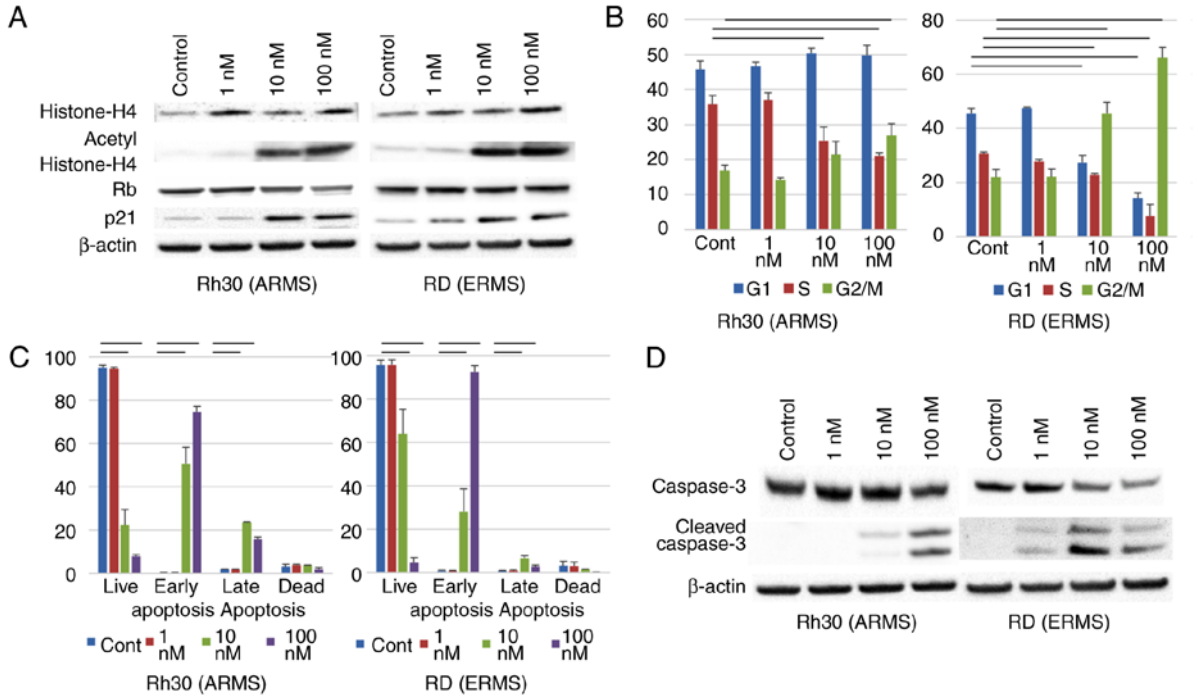


Figure 2. OBP-801 induces G2/M-phase arrest and apoptosis in ARMS and ERMS cells. (A) Western blotting of the lysates of the cells treated for 24 h with OBP-801 at the indicated concentrations for acetylated histone H4, total histone H4, Rb, and p21. β-actin is displayed as a loading control. (B) Cell cycle analysis (by flow cytometry) of Rh30 (ARMS) and RD (ERMS) cells treated with the indicated concentrations of OBP-801 for 24 h. The bars indicate the mean ± SD of triplicate independent experiments. The black line shows a significant difference (P<0.05). (C) We analyzed apoptosis in Rh30 and RD cells treated with the indicated concentrations of OBP-801 for 48 h. Annexin V-positive cells were counted as apoptotic. The bars indicate the mean ± SD of triplicate independent experiments. The black line shows a significant difference (P<0.05). (D) Western blotting of the lysates of cells treated for 24 h with the indicated concentrations of OBP-801 for total and cleaved caspase-3. β-actin is displayed as a loading control. ARMS, alveolar RMS; ERMS, embryonal RMS.

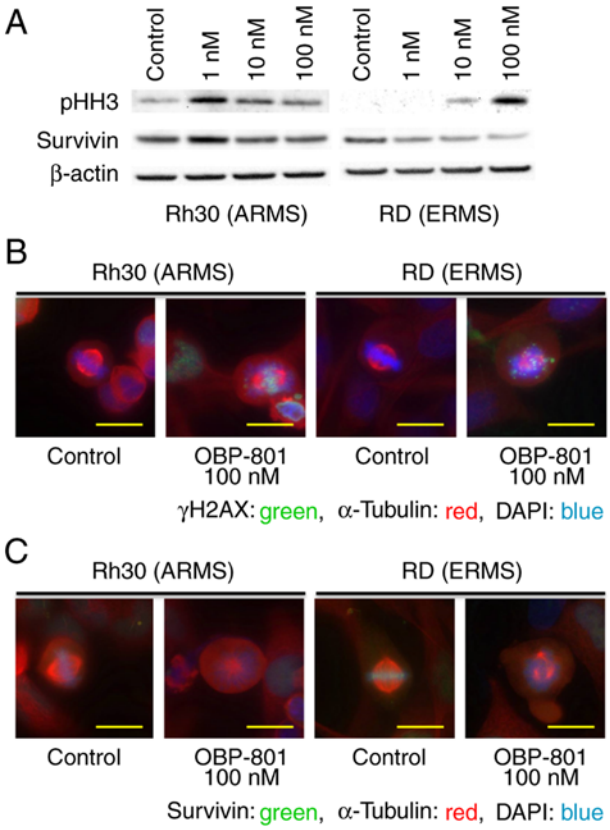


Figure 3. OBP-801 induces RMS cell death by promoting mitotic catastrophe. (A) Western blotting of the lysates of Rh30 (ARMS) and RD (ERMS) cells treated for 24 h with the indicated concentrations of OBP-801 for phospho-histone H3 (pHH3) and survivin. β-actin is displayed as a loading control. (B and C) Immunofluorescence analysis of γH2AX, survivin, and α-tubulin in Rh30 or RD cells in metaphase after OBP-801 treatment. Scale bar, 20 $\mu$m. ARMS, alveolar RMS; ERMS, embryonal RMS.

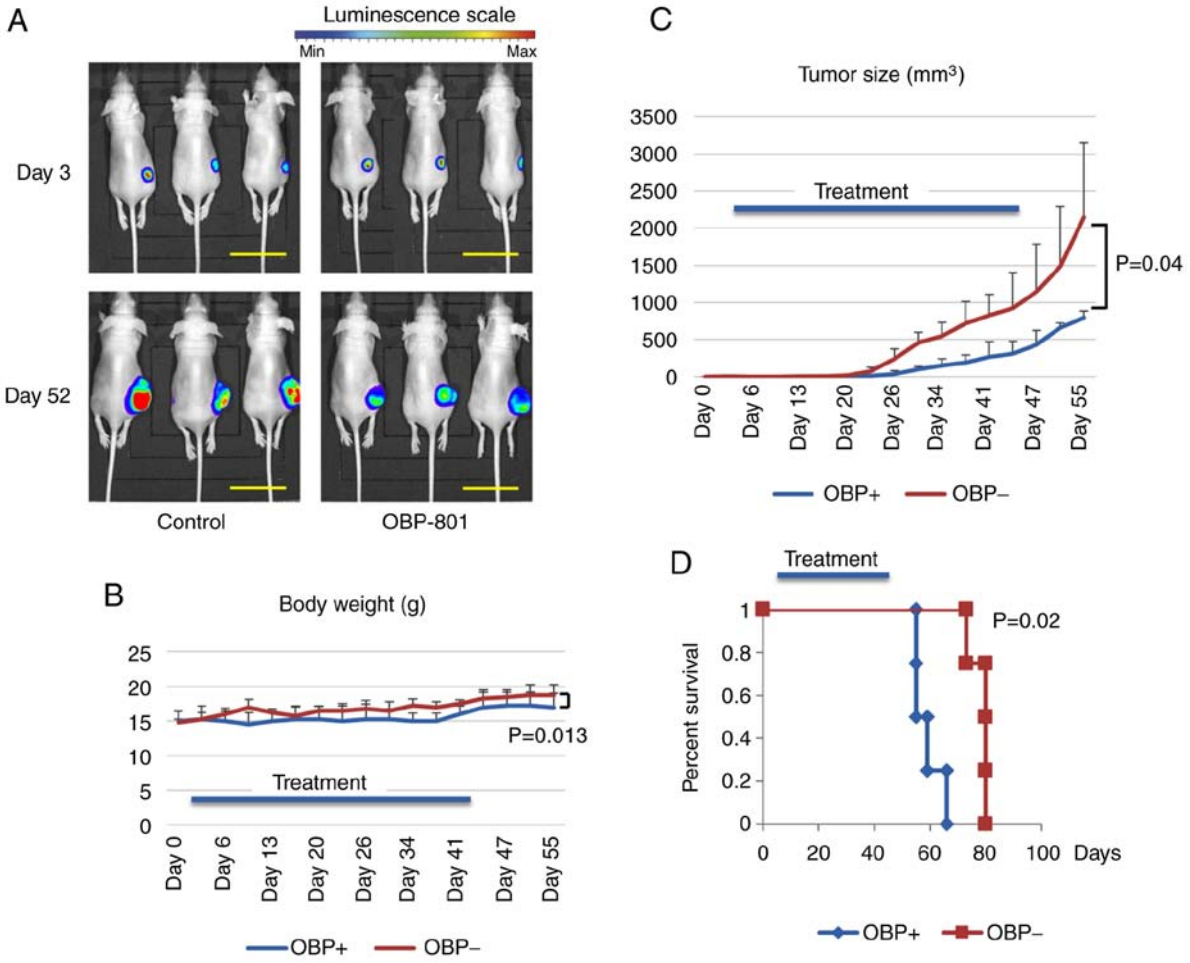


Figure 4. OBP-801 inhibits ARMS tumor growth and improvs survival *in vivo*. (A) Six mice xenografted with luciferase-positive Rh30 cells were treated with vehicle or OBP-801 (10 mg/kg) for 6 weeks, starting on day 3 after tumor injection. We measured tumor-derived bioluminescence starting 3 days after beginning the treatment. Scale bar, 3.0 cm (B and C) Effect of OBP-801 on tumor growth and body weight in nude mice with subcutaneous xenografted RMS tumors (Rh30). Points indicate the mean tumor volumes or body weights (n=4); bars, SD. (D) Kaplan-Meier survival curve of xenografted mice treated with vehicle or OBP-801.

*OBP-801 induces cell cycle arrest and apoptosis in RMS cell lines*. To evaluate the extent of HDAC inhibition in RMS cells, we performed immunoblot analyses using anti-acetylated histone antibodies. After 24 h, OBP-801 induced the accumulation of acetylated histone H4 in a concentration-dependent fashion (Fig. 2A). OBP-801 also induced p21waf1/Cip1 in a concentration-dependent manner, and hypophosphorylation of Rb in ARMS, but not in ERMS cells (Fig. 2A). We observed that OBP-801 (10 nM, 24 h) induced arrest in the G1 and G2/M-phases in ARMS cells and in the G2/M-phase in ERMS cells (Fig. 2B). In addition, OBP-801 induced cell death in RMS cells (Fig. 1B). OBP-801 (10 nM) induced early and late apoptosis in RMS cells 48 h after the treatment, as indicated by Annexin V staining assessed by flow cytometry (Fig. 2C). Treatment with OBP-801 also led to the expression of cleaved caspase-3 in a concentration-dependent manner (Fig. 2D).

*OBP-801 causes RMS cell death via mitotic catastrophe*. To examine if OBP-801 caused G2- or M-phase arrest, we immunoblotted with an antibody against phospho-histone H3, a marker of mitosis. Cells treated with OBP-801 had higher phosphorylation levels of histone H3 than control cells 24 h after the treatment; the effect was concentration-dependent (Fig. 3A). We next analyzed the nuclear morphology of RMS cells with OBP-801 treatment. We found that control cells exhibited normal chromosome distribution in metaphase, with correctly formed mitotic spindles. However, upon treatment with OBP-801, dividing RMS cells exhibited aberrant metaphase morphologies: their chromosomes were not aligned at the metaphase plate, they had an abnormal mitotic spindle distribution, survivin was not recruited to the centromeres, and exhibited lower levels of survivin than that in control cells (Fig. 3B and C); OBP-801 affected the abundance of survivin in a dose-dependent manner (Fig. 3A). In addition, OBP-801-treated RMS cells were stained with the γH2AX antibody, which indicated that they entered mitosis with damaged DNA (Fig. 3C).

*OBP-801 inhibits ARMS tumor growth in vivo and improves the survival of tumor-bearing mice*. We measured the bioluminescence from Rh30 cells in nude mice at days 3 and 52 after injection and found that the mice that had received OBP-801 had lower tumor-related bioluminescence intensities at day 52 (Fig. 4A). The mice in the drug-treated group had smaller tumors and survived longer than those in the control group (Fig. 4C and D). We did not observe statistically significant differences between the body weights of the mice in the drug-treated and control groups, indicating that the drug did not cause toxicity (Fig. 4B).

## Discussion

We used a new HDAC inhibitor, OBP-801, as a potential therapeutic drug for treating RMS. HDAC inhibitor-induced cell death is tumor-selective, as previously described (23,24). The $IC_{50}$ values of OBP-801 that we observed for ERMS cells were very low compared with the concentration required to induce notable toxic effects in normal human fibroblasts (30 $\mu$M) (18). The lack of apparent cytotoxic effects in our mouse tumor model supports the tumor-selectivity of OBP-801.

The cyclin-dependent kinase inhibitor, p21, a regulator of cellular proliferation via G1 arrest, is a crucial target for HDAC inhibitors (25,26). In this study, we confirmed that OBP-801 increased the protein level of p21 Waf1/Cip1 in a concentration-dependent manner in RMS cells, possibly via the induction of p21 mRNA. Notably, however, M-phase arrest was predominant than G1- and G2-phase arrest. These findings indicated that OBP-801 may induce arrest of M-phase followed by cell death in RMS cells.

Based on our observation that OBP-801 induced cell arrest of M-phase followed by apoptosis in RMS cells, we investigated whether apoptosis was associated with mitotic catastrophe. Mitotic catastrophe is a regulated antitumor mechanism that disrupts the survival and/or proliferation of cells that are unable to undergo complete mitosis due to unrecoverable DNA damage and that have mitotic machinery problems, and/or have a failure at mitotic checkpoints (27-29). Recently, relationships were reported between HDACs and mitotic arrest/catastrophe via DNA damage (30) and between Aurora B kinase activity (31) and Eg5 acetylation (32). Mitotic catastrophe is assessed based on unique morphological nuclear changes, such as multinucleation, macronucleation, and micronucleation. We found that OBP-801 treatment of dividing RMS cells induced γH2AX-positive aberrant metaphase morphologies, concurrent with lower levels and misalignment of survivin. Recently, Aljaberi *et al* reported that the activity of survivin in mitosis was regulated by cyclical acetylation and deacetylation during mitosis (33), which may explain how an HDAC inhibitor could induce mitotic arrest via survivin in a manner consistent with our results. These results indicated that OBP-801 may induce apoptosis in RMS cells via mitotic catastrophe.

In conclusion, to the best of our knowledge, this is the first study revealing that treatment of RMS cells with the novel HDAC inhibitor OBP-801 induced M-phase arrest followed by apoptosis via mitotic catastrophe. These results indicated that OBP-801 may be promising for the treatment of RMS. We believe that this drug should be chosen for future clinical trials.

## Acknowledgements

The authors acknowledge Peter J. Houghton M.D. (Greehey Children's Cancer Research Institute, University of Texas Health Science Center at San Antonio) for the cell lines (Rh30, Rh41, Rh3, Rh4, Rh18 and Rh28) and Naoki Kakazu M.D. (Department of Environmental and Preventive Medicine, Shimane University School of Medicine, Shimane, Japan) for cell line RMS-YM.

## Funding

The present study was supported by JSPS KAKENHI grant no. JP26461591, JSPS KAKENHI grant no. JP25253095, and the Health Labour Sciences Research grant no. 17ck0106333 h.

## Availability of data and materials

All the data supporting the conclusions of this article are included in the article.

## Authors' contributions

CT, KK, TI and HH conceived and designed this study. Experimental methodology was developed by KK, SY, MM, KT, TI, TS and HH. Experimental procedures were carried out by CT, DK and KK. All authors participated in the analysis and interpretation of data. CT and KK performed the statistical analysis and wrote the manuscript. All authors read and approved the manuscript and agree to be accountable for all aspects of the research in ensuring that the accuracy or integrity of any part of the work are appropriately investigated and resolved.

## Ethics approval and consent to participate

The present study was approved by the Committee for Animal Research of Kyoto Prefectural University of Medicine (permission no. M27-477).

## Patient consent for publication

Not applicable.

## Competing interests

The authors declare that they have no competing interests.

## References

1. Merlino G and Helman LJ: Rhabdomyosarcoma-working out the pathways. Oncogene 18: 5340-5348, 1999.
2. Davicioni E, Anderson MJ, Finckenstein FG, Lynch JC, Qualman SJ, Shimada H, Schofield DE, Buckley JD, Meyer WH, Sorensen PH, *et al*: Molecular classification of rhabdomyosarcoma-genotypic and phenotypic determinants of diagnosis: A report from the Children's Oncology Group. Am J Pathol 174: 550-564, 2009.
3. Kikuchi K, Soundararajan A, Zarzabal LA, Weems CR, Nelon LD, Hampton ST, Michalek JE, Rubin BP, Fields AP and Keller C: Protein kinase C iota as a therapeutic target in alveolar rhabdomyosarcoma. Oncogene 32: 286-295, 2013.
4. Miyachi M, Kakazu N, Yagyu S, Katsumi Y, Tsubai-Shimizu S, Kikuchi K, Tsuchiya K, Iehara T and Hosoi H: Restoration of p53 pathway by nutlin-3 induces cell cycle arrest and apoptosis in human rhabdomyosarcoma cells. Clin Cancer Res 15: 4077-4084, 2009.
5. Sokolowski E, Turina CB, Kikuchi K, Langenau DM and Keller C: Proof-of-concept rare cancers in drug development: The case for rhabdomyosarcoma. Oncogene 33: 1877, 2014.
6. Minucci S and Pelicci PG: Histone deacetylase inhibitors and the promise of epigenetic (and more) treatments for cancer. Nat Rev Cancer 6: 38-51, 2006.
7. Bolden JE, Peart MJ and Johnstone RW: Anticancer activities of histone deacetylase inhibitors. Nat Rev Drug Discov 5: 769-784, 2006.

8. Khabele D, Son DS, Parl AK, Goldberg GL, Augenlicht LH, Mariadason JM and Montgomery RV: Drug-induced inactivation or gene silencing of class I histone deacetylases suppresses ovarian cancer cell growth: implications for therapy. Cancer Biol Ther 6: 795-801, 2007.
9. Strait KA, Warnick CT, Ford CD, Dabbas B, Hammond EH and Ilstrup SJ: Histone deacetylase inhibitors induce $G_2$-checkpoint arrest and apoptosis in cisplatinum-resistant ovarian cancer cells associated with overexpression of the Bcl-2-related protein Bad. Mol Cancer Ther 4: 603-611, 2005.
10. Khan O and La Thangue NB: HDAC inhibitors in cancer biology: Emerging mechanisms and clinical applications. Immunol Cell Biol 90: 85-94, 2012.
11. West AC and Johnstone RW: New and emerging HDAC inhibitors for cancer treatment. J Clin Invest 124: 30-39, 2014.
12. Porcu P and Wong HK: We should have a dream: Unlocking the workings of the genome in cutaneous T-cell lymphomas. Clin Lymphoma Myeloma 9: 409-411, 2009.
13. Mann BS, Johnson JR, Cohen MH, Justice R and Pazdur R: FDA approval summary: Vorinostat for treatment of advanced primary cutaneous T-cell lymphoma. Oncologist 12: 1247-1252, 2007.
14. Jain S and Zain J: Romidepsin in the treatment of cutaneous T-cell lymphoma. J Blood Med 2: 37-47, 2011.
15. Blattmann C, Oertel S, Ehemann V, Thiemann M, Huber PE, Bischof M, Witt O, Deubzer HE, Kulozik AE, Debus J, *et al*: Enhancement of radiation response in osteosarcoma and rhabdomyosarcoma cell lines by histone deacetylase inhibition. Int J Radiat Oncol Biol Phys 78: 237-245, 2010.
16. Kutko MC, Glick RD, Butler LM, Coffey DC, Rifkind RA, Marks PA, Richon VM and LaQuaglia MP: Histone deacetylase inhibitors induce growth suppression and cell death in human rhabdomyosarcoma in vitro. Clin Cancer Res 9: 5749-5755, 2003.
17. Abraham J, Nuñez-Álvarez Y, Hettmer S, Carrió E, Chen HI, Nishijo K, Huang ET, Prajapati SI, Walker RL, Davis S, *et al*: Lineage of origin in rhabdomyosarcoma informs pharmacological response. Genes Dev 28: 1578-1591, 2014.
18. Shindoh N, Mori M, Terada Y, Oda K, Amino N, Kita A, Taniguchi M, Sohda KY, Nagai K, Sowa Y, *et al*: YM753, a novel histone deacetylase inhibitor, exhibits antitumor activity with selective, sustained accumulation of acetylated histones in tumors in the WiDr xenograft model. Int J Oncol 32: 545-555, 2008.
19. Kubo K, Naoe T, Utsumi KR, Ishiguro Y, Ueda K, Shiku H and Yamada K: Cytogenetic and cellular characteristics of a human embryonal rhabdomyosarcoma cell line, RMS-YM. Br J Cancer 63: 879-884, 1991.
20. Kikuchi K, Tsuchiya K, Otabe O, Gotoh T, Tamura S, Katsumi Y, Yagyu S, Tsubai-Shimizu S, Miyachi M, Iehara T, *et al*: Effects of PAX3-FKHR on malignant phenotypes in alveolar rhabdomyosarcoma. Biochem Biophys Res Commun 365: 568-574, 2008.
21. Kikuchi K, Hettmer S, Aslam MI, Michalek JE, Laub W, Wilky BA, Loeb DM, Rubin BP, Wagers AJ and Keller C: Cell-cycle dependent expression of a translocation-mediated fusion oncogene mediates checkpoint adaptation in rhabdomyosarcoma. PLoS Genet 10: e1004107, 2014.
22. Nishijo K, Hosoyama T, Bjornson CR, Schaffer BS, Prajapati SI, Bahadur AN, Hansen MS, Blandford MC, McCleish AT, Rubin BP, *et al*: Biomarker system for studying muscle, stem cells, and cancer in vivo. FASEB J 23: 2681-2690, 2009.
23. Marks PA, Richon VM, Miller T and Kelly WK: Histone deacetylase inhibitors. Adv Cancer Res 91: 137-168, 2004.
24. Ungerstedt JS, Sowa Y, Xu WS, Shao Y, Dokmanovic M, Perez G, Ngo L, Holmgren A, Jiang X and Marks PA: Role of thioredoxin in the response of normal and transformed cells to histone deacetylase inhibitors. Proc Natl Acad Sci USA 102: 673-678, 2005.
25. Zupkovitz G, Grausenburger R, Brunmeir R, Senese S, Tischler J, Jurkin J, Rembold M, Meunier D, Egger G, Lagger S, *et al*: The cyclin-dependent kinase inhibitor p21 is a crucial target for histone deacetylase 1 as a regulator of cellular proliferation. Mol Cell Biol 30: 1171-1181, 2010.
26. Bose P, Dai Y and Grant S: Histone deacetylase inhibitor (HDACI) mechanisms of action: Emerging insights. Pharmacol Ther 143: 323-336, 2014.
27. Galluzzi L, Vitale I, Aaronson SA, Abrams JM, Adam D, Agostinis P, Alnemri ES, Altucci L, Amelio I, Andrews DW, *et al*: Molecular mechanisms of cell death: recommendations of the Nomenclature Committee on Cell Death 2018. Cell Death Differ 25: 486-551, 2018.
28. Castedo M, Perfettini JL, Roumier T, Andreau K, Medema R and Kroemer G: Cell death by mitotic catastrophe: A molecular definition. Oncogene 23: 2825-2837, 2004.
29. Vitale I, Galluzzi L, Castedo M and Kroemer G: Mitotic catastrophe: a mechanism for avoiding genomic instability. Nat Rev Mol Cell Biol 12: 385-392, 2011.
30. Cornago M, Garcia-Alberich C, Blasco-Angulo N, Vall-Llaura N, Nager M, Herreros J, Comella JX, Sanchis D and Llovera M: Histone deacetylase inhibitors promote glioma cell death by G2 checkpoint abrogation leading to mitotic catastrophe. Cell Death Dis 5: e1435, 2014.
31. Li Y, Kao GD, Garcia BA, Shabanowitz J, Hunt DF, Qin J, Phelan C and Lazar MA: A novel histone deacetylase pathway regulates mitosis by modulating Aurora B kinase activity. Genes Dev 20: 2566-2579, 2006.
32. Nalawansha DA, Gomes ID, Wambua MK and Pflum MKH: HDAC inhibitor-induced mitotic arrest ss mediated by Eg5/KIF11 acetylation. Cell Chem Biol 24: 481-492, 2017.
33. Aljaberi AM, Webster JR and Wheatley SP: Mitotic activity of survivin is regulated by acetylation at K129. Cell Cycle 14: 1738-1747, 2015.